ROYAL SOCIETY
OF CHEMISTRY

PAPER

Check for updates

A novel fullerene-lysine derivative with noticeable ROS scavenging capabilities for improving type 2 diabetes mellitus

Jiaqi Weng,†[bc] Wei Guo,†[ab] Jie Liu,†[ab] Kollie Larwubah,[a] Jianjun Guo,[ab] Yanrong Jia*[c] and Meilan Yu (ID) *[ab]

As some of the most promising candidates available, fullerene-derived bioactive agents have been explored as new drugs with high efficacy and safety for biomedical applications. In this study, a fullerene-lysine derivative (C_{60}-Lys) was synthesized successfully and proved to be good at treating type 2 diabetes mellitus (T2DM). C_{60}-Lys could alleviate oxidative stress both in streptozotocin (STZ)-induced MIN6 cells and in STZ-induced T2DM mice subjected to a high-fat diet, and it significantly normalized glucose uptake and reduced blood glucose. In addition, C_{60}-Lys can alleviate insulin resistance, hyperinsulinemia and lipid levels in T2DM mice. It was further confirmed that C_{60}-Lys could alleviate oxidative stress by increasing the activities of antioxidant enzymes and stabilizing the mitochondrial membrane potential (MMP) of pancreatic β-cells to reduce the overproduction of ROS. The results provide compelling evidence that C_{60}-Lys possesses promising applications for T2DM treatment.

Introduction

As a non-communicable disease associated with systemic metabolic disorders, T2DM has attracted much attention regarding its etiology and corresponding treatment plans. Currently, T2DM affects 437 million people worldwide.[1] T2DM causes myriad pathologies in many organ systems, which is not unexpected as it causes significant abnormalities in almost all metabolic pathways of cells. These complications are responsible for most of the morbidity and mortality associated with the disease.[2] The risk of all-cause mortality for individuals with type 2 diabetes mellitus (T2DM) is 1.8 times greater than that for individuals without T2DM, and the medical expenses associated with T2DM are 2.3 times higher than those for individuals without the condition.[3]

It was reported that the etiology of T2DM includes pancreatic β-cell dysfunction and insulin resistance.[4–6] Among these, pancreatic β-cell dysfunction is the most critical pathophysiological feature and determinant of T2DM.[7] When insulin resistance occurs, downstream peripheral tissue begins to react with insulin, and it cannot produce a normal coordinated hypoglycemic response; then, the blood sugar level increases. To keep the blood sugar stable, pancreatic β-cells will compensate through the secretion of excessive insulin,[8] which can lead to the occurrence of intracellular endoplasmic reticulum stress (ERS) in pancreatic β-cells.[9] Severe ERS also promotes the production of reactive oxygen species (ROS),[10] which leads to pancreatic β-cell dysfunction and cell apoptosis.[11] Huang *et al.*[12] reported that SENDs greatly rescue β-cells by restoring mitophagy and alleviating endoplasmic reticulum stress.

Many studies have shown that oxidative stress is the main pathogenic mechanism of diabetes.[13] Oxidative stress is the main upstream event in the development of diabetic complications and insulin resistance, and pancreatic β-cells are very sensitive to ROS due to relatively low levels of antioxidant enzymes in β-cells, so this can directly damage pancreatic β-cells and promote apoptosis.[14] When the body perceives an insulin deficiency, the over-proliferative secretion of pancreatic β-cells does not meet the body's demand for insulin, and the excessive mitochondrial activity caused by persistent hyperglycemia leads to a large increase in ROS, which exceeds the antioxidant capacity of β-cells; the body then experiences oxidative stress with an inflammatory response, leading to pancreatic β-cell dysfunction.[15] Therefore, the development of insulin resistance can lead to pancreatic β-cell dysfunction. Apoptosis and a lack of compensational regeneration of pancreatic β-cells,[16] which is pancreatic β-cell dysfunction, can lead to the development of chronic hyperglycemia. Chronic hyperglycemia leads to apoptosis triggering and cell de-differentiation in turn, eventually making a vicious cycle.[17]

[a]College of Life Science and Medicine, Zhejiang Sci-Tech University, Hangzhou 310018, China. E-mail: gw980310@163.com; kaki0925@yeah.net; larwubahkollie@gmail.com; biojjguo@zstu.edu.cn; meilanyu@zstu.edu.cn

[b]Shaoxing Academy of Biomedicine, Zhejiang Sci-Tech University, Shaoxing 312030, China

[c]School of Chemistry and Chemical Engineering, Zhejiang Sci-Tech University, Hangzhou 310018, China. E-mail: 1174760663@qq.com; jiayr102518@163.com

† These authors contributed equally to this work.

Thus, it would be meritorious to develop one novel drug to lower blood glucose and improve metabolic dysfunction with low toxic side effects. Hence, it is still pressing to develop novel efficient biomaterials with adequate anti-diabetic efficacy, that can improve metabolic dysfunction, and have low toxicity.

C_{60} and its derivatives are widely used due to their excellent free radical scavenging abilities and antioxidant properties in the fields of hepatoprotection,[18] neuroprotection[19] and tumor therapy.[20] They have also been used to protect cellular mitochondria, repair damaged organs from oxidative stress, and attenuate inflammatory responses. One molecule of fullerene can react with multiple molecules of reactive oxygen species to achieve a good ROS scavenging effect.[21] However, how fullerene balances blood sugar levels and the specific mechanisms of T2DM in response to fullerene have not been fully clarified. Some common clinical medications, such as sulfonylureas, biguanides, α-glucosidase inhibitors, thiazolidinediones and so on,[22–25] are unsatisfactory due to several adverse outcomes, including the need for long-term medication, continuous weight gain, the impairment of renal function, and the onset of pancreatitis.[26] Therefore, C_{60} modified with efficient and highly clinically effective biomaterial components was designed and prepared. Su *et al.* found that the oral delivery of C_{60} could reduce intestinal inflammation in both the ileum and colon of mice caused by a long-term high-fat diet.[27] Wang *et al.* reported the use of dicarboxy fullerene modified with mannose (DCFM) as an immunomodulator to actively polarize TAMs and boost antitumor immunity.[28]

Herein, C_{60}-Lys was prepared as a potential therapeutic agent to improve the oxidative stress levels of pancreatic β-cells and restore the function of pancreatic tissue by utilizing its excellent antioxidant properties, which will provide a reference to find and develop novel drugs for the treatment of T2DM.

Materials and methods

Materials

Solid C_{60} (99% purity) was obtained from Xiamen Funano Co. Ltd, Fujian, China; streptozotocin (STZ), dimethyl sulfoxide (DMSO), citric acid and sodium citrate were purchased from Macklin Biochemical Co. Ltd, Shanghai, China; Thiazolyl Blue (MTT), trypsin–EDTA solution, metformin hydrochloride, D-glucose and 0.9% normal saline were purchased from Solarbio Science & Technology Co. Ltd, Beijing, China; human insulin injections were obtained from Wanbang Pharmaceutical Co. Ltd, Jiangsu, China.

Synthesis and characterization of C_{60}-Lys

C_{60}-Lys was prepared by a nucleophilic addition reaction, and the modification steps are as follows. Firstly, 110 mg of C_{60} was completely dispersed in 70 mL of toluene and named solution A; then 5.6 g of L-lysine and 1.7 g of NaOH were dissolved in 6 mL of water, and 40 mL of ethanol was added to dissolve them completely, forming solution B. Subsequently, solution A was added dropwise into solution B, and the mixed solution was reacted at 50 °C for 24 h. The lower brown-black hydro-alcoholic mixed phase was separated by a partition funnel, extraction, concentration under reduced pressure, ethanol precipitation, centrifugation and vacuum drying: a brown-black solid powder was obtained. C_{60}-Lys was characterized by Fourier transform infrared spectroscopy (FT-IR, Nicolet iN10 MX, Thermo, USA) and dynamic light scattering (DLS, Malvern, UK).

Cell cultures

MIN6 cells were obtained from the Shanghai Institute of Cell Biology, Chinese Academy of Sciences (Shanghai, China). MIN6 cells were incubated with RPMI-1640 medium (Gibco, USA) culture medium supplemented with 10% fetal bovine serum (FBS, Excell, China) and 1% penicillin-streptomycin solution (Beyotime, China) in 5% CO_2 at 37 °C in a humidified incubator.

Cell viability assays

Cell viability was evaluated using Thiazolyl Blue (MTT, Solarbio, China) after treatment with STZ and C_{60}-Lys at different concentrations; the treatment concentrations and treatment times are shown in Table 1. Then, cell viability was evaluated according to the manufacturer instructions.

Apoptosis and cell cycle assays

Cells were treated with STZ and C_{60}-Lys individually. Cell apoptosis was assessed using an Annexin V-FITC/PI apoptosis assay kit (Vazyme, China) and cell cycle was assessed using a cell cycle assay kit (Beyotime, China) according to the instructions.

Oxidative stress marker testing

The levels of mitochondrial ROS were evaluated with a flow cytometer (Accuri C6 Plus, USA) using a ROS assay kit (Solarbio, China). The levels of superoxide dismutase (SOD) were evaluated by spectrophotometry (UV2700, Japan) using a total superoxide dismutase assay kit (Beyotime, China) according to the instructions.

Cellular mitochondrial membrane potential detection

The cellular MMP levels were measured using an enhanced mitochondrial membrane potential assay kit (Beyotime, China) according to the instructions.

Glucose uptake and insulin secretion

The glucose uptake of cells was measured using a glucose assay kit (Beyotime, China) according to the instructions. In this study, the content of extracellular glucose was measured to indirectly reflect the uptake of glucose by the MIN6 cells. The

Table 1 The concentrations and durations of drug treatment

Treatment drug	Treatment concentration/mM	Treatment time/h
STZ	0, 0.5, 1, 2, 5	1, 2, 4, 6
C_{60}-Lys	0, 10, 20, 50	24, 48, 72

insulin secretion of cells was measured using a mouse insulin ELISA Kit (Solarbio, China) according to the instructions. All samples were cell supernatant samples. Finally, the cells were normalized using BSA protein quantification.

Animal experiments

Five-week-old male mice were obtained from Hangzhou Hangs Biotechnology Co. Ltd (C57BL/6N). They were housed in a temperature-controlled, ventilated, and standardized animal room and had free access to food (normal rodent chow) and water in the Experimental Animal Center of Zhejiang Sci-Tech University. All animal procedures were performed in accordance with the Guidelines for Care and Use of Laboratory Animals of Zhejiang Sci-Tech University and approved by the Animal Ethics Committee of Zhejiang Sci-Tech University.

The experiments were started when mice were 6 weeks old; after 1 week of adaption, mice were randomly divided into a control group ($n = 7$) and a high-fat diet group ($n = 40$). Mice in the control group consumed 10% fat (Research Diets, Inc., USA) and were injected with the corresponding volume of citrate buffer for 5 consecutive days. In the high-fat diet group, animals consumed a diet consisting of 60% fat, followed by the induction of diabetes through the intraperitoneal injection of STZ ($30\ mg\ kg^{-1}\ day^{-1}$) for 5 consecutive days. After that, model construction was carried out by measuring the fasting blood glucose level and insulin tolerance, then the model group was divided into five groups based on body weight and fasting blood glucose.

The mice were divided into 5 groups as follows: (1) control, 10% fat caloric control diet + saline, $n = 7$; (2) T2DM, 60% fat caloric high-fat diet + saline, $n = 7$; (3) T2DM + C_{60}-Lys(H), 60% fat caloric high-fat diet + C_{60}-Lys ($8\ \mu g\ kg^{-1}\ day^{-1}$), $n = 7$; (4) T2DM + C_{60}-Lys(L), 60% fat caloric high-fat diet + C_{60}-Lys ($4\ \mu g\ kg^{-1}\ day^{-1}$), $n = 7$; and (5) T2DM + metformin, 60% fat caloric high-fat diet + metformin ($100\ mg\ kg^{-1}\ day^{-1}$), $n = 7$. Food and water intakes were recorded during the feeding period. The mice were all sacrificed for further study on the 28th day. Blood was obtained from the eye socket, and tissue samples were collected, weighed, and preserved as soon as possible. Some tissue samples were fixed in 4% formalin at once, and some tissue samples were immediately iced in liquid nitrogen and stored at $-80\ °C$.

IPGTT and IPITT

After injecting drugs for 28 days, intraperitoneal glucose tolerance testing (IPGTT) was conducted. The mice fasted for 16 h and then were injected with glucose at a dose of $1\ g\ kg^{-1}$. The blood glucose was measured by tail snipping 0, 15, 30, 60, 90 and 120 min after the initial glucose loading. In intraperitoneal insulin tolerance testing (IPITT), mice fasted for 6 h, and then human biosynthetic insulin was injected intraperitoneally at a dose of $0.8\ U\ kg^{-1}$, and the blood glucose was measured after 0, 15, 30, 60 and 120 min. The blood glucose of mice was measured using a glucometer (Roche ACCU-CHEK, Germany). The AUC values of the glucose concentrations were calculated.

Determination of biochemical parameters

Blood samples were collected from the eye socket before sacrifice, and serum was acquired after centrifugation at 4000 rpm for 10 min. Insulin levels were measured using a mouse insulin ELISA kit (Solarbio, China) according to the instructions. The oxidative stress-related indicators (SOD, catalase (CAT), and malondialdehyde (MDA)) were analyzed spectrophotometrically using diagnostic reagent kits (Nanjing Jiancheng Bioengineering Institute, China). The two levels of lipids were measured using the kit for TG/TC assay (Purebio, China) according to the instructions. The insulin resistance index homeostasis model assessment of insulin resistance (HOMA-IR), insulin sensitivity index insulin secretion of homeostasis model assessment (HOMA-IS), and pancreatic β-cell function index homeostasis model assessment-β (HOMA-β) values are calculated as shown below: HOMA-IR = FBG × FINS/22.5; HOMA-IS = 20 × FINS/(FBG-3.5); and HOMA-β = 1/(log FINS × log FINS), where FBG is the fasting blood glucose of mice ($mmol\ L^{-1}$) and FINS is the fasting insulin of mice ($\mu IU\ mL^{-1}$).

Histopathological examination of pancreases

The pancreatic tissue of mice was fixed with 4% paraformaldehyde fix solution for more than 24 h, then the fix solution was removed and dehydrated. Subsequently, the tissue was immersed in paraffin for 3 h, and the paraffin-soaked tissue was taken out for embedding. The tissue was embedded and sectioned, with a thickness of about 4 μm. After cutting, it was flattened in 40 °C warm water, baked in an oven at 60 °C for 2 h, and then the slices were stored at room temperature. Paraffin slices were baked again in an oven at 60 °C for 2 h, followed by dewaxing and hydration. The slices were first stained with hematoxylin stain for 5 min and then rinsed with tap water, followed by eosin stain for 5–8 s and then rinsing with running water. Subsequently, the slices were dehydrated again, and finally the slices were taken out and sealed with neutral resin. The H&E-stained slices were placed under a microscope for microscopic examination, where the nucleus was blue and the cytoplasm was red.

RNA extraction and gene expression analysis by RT-qPCR

Total RNA was extracted from MIN6 cells and mouse pancreas tissue samples with an RNA-Quick Purification kit (Esunbio, China). Besides, reverse transcription was performed with a ReverTra Ace qPCR RT kit (TOYOBO, Japan) according to the manufacturer's instructions. Quantitative real-time PCR (RT-qPCR) was performed using a Taq Pro Universal SYBR qPCR Master Mix kit (Vazyme, China) according to the manufacturer's instructions. All reactions were performed in triplicate. The reaction program of RT-qPCR was as follows: 95 °C for 30 s, followed by 40 cycles of 95 °C for 10 s, 60 °C for 30 s, and 72 °C for 15 s, with fluorescence signals collected at 72 °C. The primers are shown in Table 2. Finally, the Ct values from the RT-qPCR results were calculated and analyzed using the comparative threshold cycle ($2^{-\Delta\Delta Ct}$) method.

Table 2 Primer sequences used

Primer name	Primer sequence (5'-3')
β-Actin-F	GGCTGTATTCCCCTCCATCG
β-Actin-R	CCAGTTGGTAACAATGCCATGT
Nrf2-F	CTGAACTCCTGGACGGGACTA
Nrf2-R	CGGTGGGTCTCCGTAAATGG
HO-1-F	TGACACCTGAGGTCAAGCAC
HO-1-R	CAGCTCCTCAAACAGCTCAATG

Data analysis

Each group of experiments was repeated three times independently, and the experimental data were expressed as means $\pm$ standard deviations. GraphPad Prism 8 software was used to make graphs, and statistical significance analysis was performed using t-tests and ANOVA; ns represents $p > 0.05$, and differences were considered statistically significant when $p < 0.05$: * represents $p < 0.05$, ** represents $p < 0.01$, and *** represents $p < 0.001$.

Results and discussion

Synthesis and characterization of C_{60}-Lys

C_{60}-Lys was synthesized after reacting the C_{60} dispersion solution and L-lysine alkaline aqueous solution at 50 °C for 24 h. A schematic diagram of the reaction is shown in Fig. 1a. The product was post-treated and some brown powder was obtained. As shown in Fig. 1b, the peaks at 3419 cm^{-1} and 2922 cm^{-1} are telescopic vibration peaks of primary amine – NH$_2$ and secondary amine –NH–, respectively, from the side chains; the characteristic peak at 2853 cm^{-1} is the telescopic vibration peak of –C–H from the side chains; the characteristic peak at 1596 cm^{-1} is the telescopic vibration peak of –C=O; and the characteristic peak at 1113 cm^{-1} is the vibrational band of –C–N– from the side chains. The characterization illustrated that the C_{60}-Lys biomaterial is very rich in functional groups, including hydroxyl (–OH), amino (–NH$_2$) and carboxyl (–COOH) groups. The presence of these groups endows C_{60}-Lys with unique physicochemical properties, which probably determines its application potential in fields such as biomedicine.

A further understanding of the particle size of the nanosystem can help predict the fate of C_{60}-Lys at the biological level.[29] In general, nanoparticles possessing a particle size below 200 nm are considered ideal for prolonged circulation due to the propensity to avoid liver uptake and avoid rapid renal clearance.[30] The measured diameter of C_{60}-Lys particles was 143.1 ± 9.0 nm (Fig. 1c). The results indicated that C_{60}-Lys, with an appropriate size and narrow particle size distribution, would be effective for biomedical applications.[29]

In vitro activity of C_{60}-Lys toward pancreatic β-cells

To investigate the effect of C_{60}-Lys on the activity of MIN6 cells injured by STZ, MIN6 cells were treated with different concentrations of C_{60}-Lys and STZ. The cell viability was detected using MTT. It was observed that C_{60}-Lys had undetectable cytotoxicity; even when the concentration of C_{60}-Lys was increased up to 50
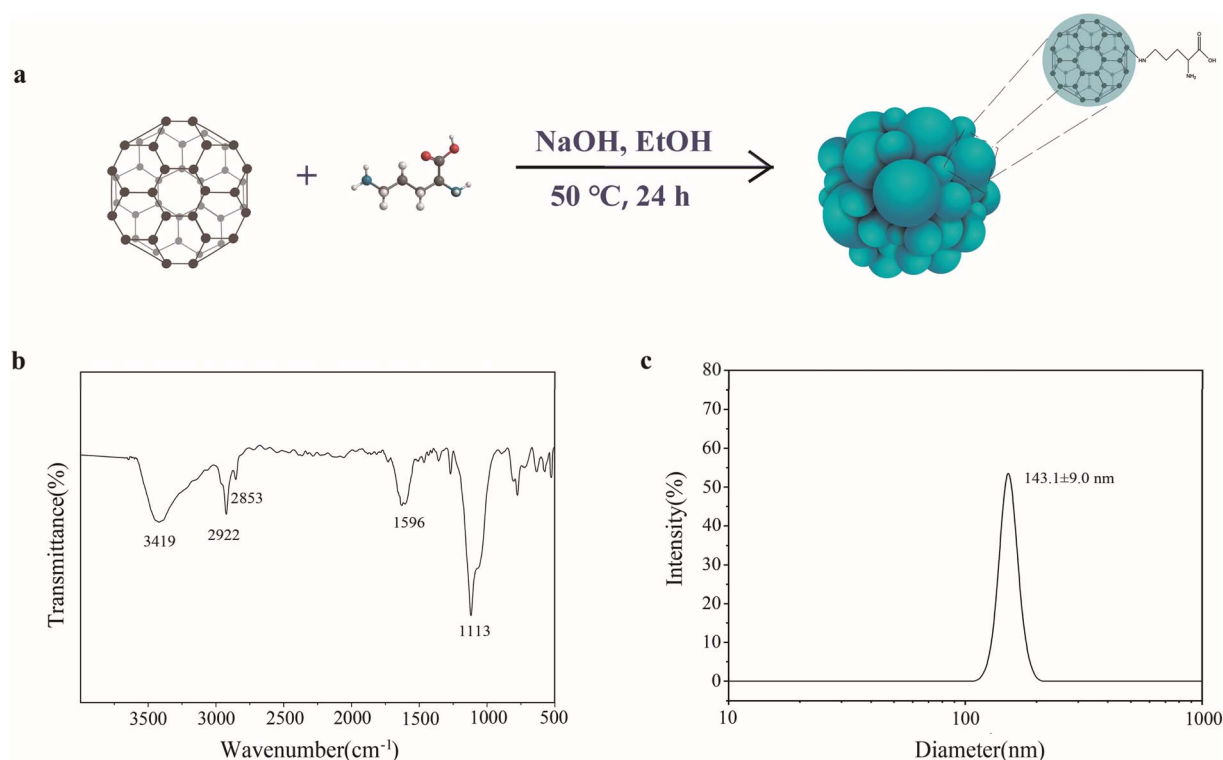

Fig. 1 (a) A schematic diagram of the preparation of C_{60}-Lys. (b) The FT-IR spectrum of C_{60}-Lys. (c) The hydrodynamic size distribution of C_{60}-Lys from DLS.
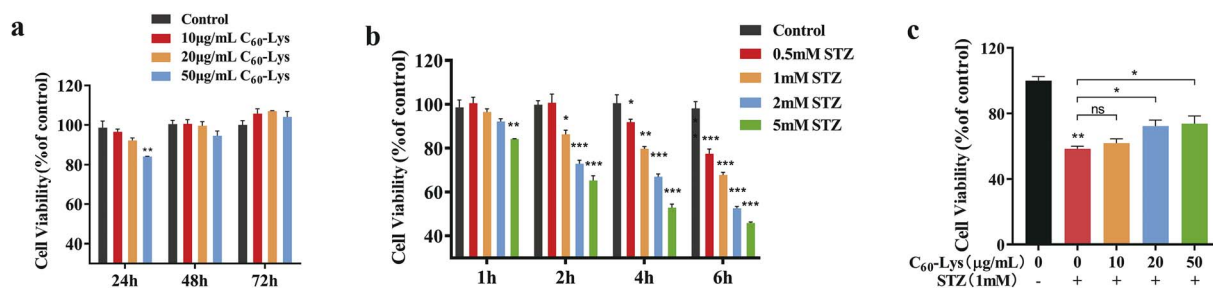
Fig. 2 Cell viability assays *in vitro*. (a): The effects of C_{60}-Lys on the viability of MIN6 cells. (b) The effects of STZ on the viability of MIN6 cells. (c) The viability of MIN6 cells after STZ pretreatment and C_{60}-Lys treatment. ns means $p > 0.05$, * means $p < 0.05$, ** means $p < 0.01$, and *** means $p < 0.001$ compared with the control group. Data were analyzed using *t*-tests and ANOVA.

μg mL^{-1}, cell survival rates exceeded 80% (Fig. 2a). The inhibitory effect on cell viability gradually enhanced with an increase in STZ concentration and induction time (Fig. 2b). After C_{60}-Lys treatment, the viability of MIN6 cells damaged by STZ showed significant improvements, as depicted in Fig. 2c. As a result, the concentration of STZ used in subsequent experiments was chosen to be 1 mM, and the induction time was chosen to be 4 h. The C_{60}-Lys treatment time was chosen to be 48 h, and low (10 μg mL^{-1}) and high (50 μg mL^{-1}) treatment concentrations of C_{60}-Lys were chosen.

Effects on apoptosis and the cell cycle of pancreatic β-cells

The apoptosis of pancreatic β-cells plays an important role in the pathophysiology of T2DM. FCM was used to investigate STZ-induced apoptosis in MIN6 cells during C_{60}-Lys fullerene nanoparticle therapy. As illustrated in Fig. 3a and b, significant cell death was observed after STZ treatment and this significantly decreased after C_{60}-Lys treatment. Specifically, the apoptotic cell proportion decreased by approximately 36.71% after treatment with 10 μg mL^{-1} C_{60}-Lys. The apoptotic cell proportion further decreased by approximately 45.84% after treatment with 50 μg mL^{-1} C_{60}-Lys. These findings suggest that C_{60}-Lys can alleviate STZ-induced apoptosis in pancreatic β-cells.

Next, further experiments were carried out to make clear whether C_{60}-Lys modulates cell cycle progress. Cell cycle assays were performed (Fig. 3c and d) where cells were treated with STZ or C_{60}-Lys or co-incubated with STZ and C_{60}-Lys. The results showed that the cell cycle of pancreatic β-cells with STZ was blocked in the G2 phase and was inhibited from entering the division phase. Under treatment from C_{60}-Lys after STZ induction, the cell cycle of the treatment group did not change. The results indicated that C_{60}-Lys can alleviate pancreatic β-cell apoptosis, but it had no effect on the cell cycle changes induced by STZ.

Regulation of glucose uptake and insulin secretion by pancreatic β-cells

The MIN6 cells were first treated with STZ and then incubated with C_{60}-Lys. The uptake of glucose by the cells is indirectly calculated by detecting the amount of extracellular glucose. As shown in Fig. 4a, after STZ treatment, the extracellular glucose

significantly increased. Compared with the STZ model group, the extracellular glucose content in the groups with the co-incubation of STZ and C_{60}-Lys was significantly lower. It was indicated that C_{60}-Lys could alleviate the decrease in the glucose uptake ability of pancreatic β-cells caused by STZ.

Then the effects on insulin secretion in MIN6 cells were tested, as shown in Fig. 4b. Compared with the control group, STZ treatment can cause a decrease in the insulin secretion ability of MIN6 cells. Meanwhile, compared with the STZ model group, the insulin content detected in the groups with the co-incubation of STZ and C_{60}-Lys was significantly increased. Thus, it was suggested that C_{60}-Lys relieves impaired insulin secretion.

The eminent pathogenic features of T2DM include pancreatic β-cell impairment and insulinemia, which ultimately results in defective insulin secretion and persistent hyperglycemia.[31] Given the above evidence, it was determined that C_{60}-Lys can cure T2DM by restoring the insulin secretory capacity and increasing the glucose uptake of pancreatic β-cells.

Regulation of ROS and SOD levels and stabilization of the MMP

Specifically, the levels of cellular ROS were evaluated using a cellular ROS detection kit; as shown in Fig. 4c and d, upon treatment with C_{60}-Lys, the ROS levels of pancreatic β-cells induced with STZ decreased significantly. This could suggest that C_{60}-Lys significantly decreased the levels of cellular ROS.

SOD is a typical antioxidant enzyme. The levels of SOD were measured using a superoxide dismutase assay kit. As shown in Fig. 4e, the levels of SOD decreased significantly after STZ treatment and were restored after C_{60}-Lys treatment. Specifically, SOD levels increased by about 90.51% after treatment with 10 μg mL^{-1} C_{60}-Lys and by about 107.54% after treatment with 50 μg mL^{-1} C_{60}-Lys. It was indicated that C_{60}-Lys significantly increased the levels of cellular SOD.

Pancreatic β-cell failure is mainly caused by mitochondrial dysfunction.[32] The cellular MMP levels were measured using an enhanced mitochondrial membrane potential assay kit. As shown in Fig. 4f and g, the MMP of pancreatic β-cells had a decrease of about 28.1% after STZ treatment, and the MMP is restored after C_{60}-Lys treatment; it is suggested that C_{60}-Lys can stabilize the MMP of pancreatic β-cells.
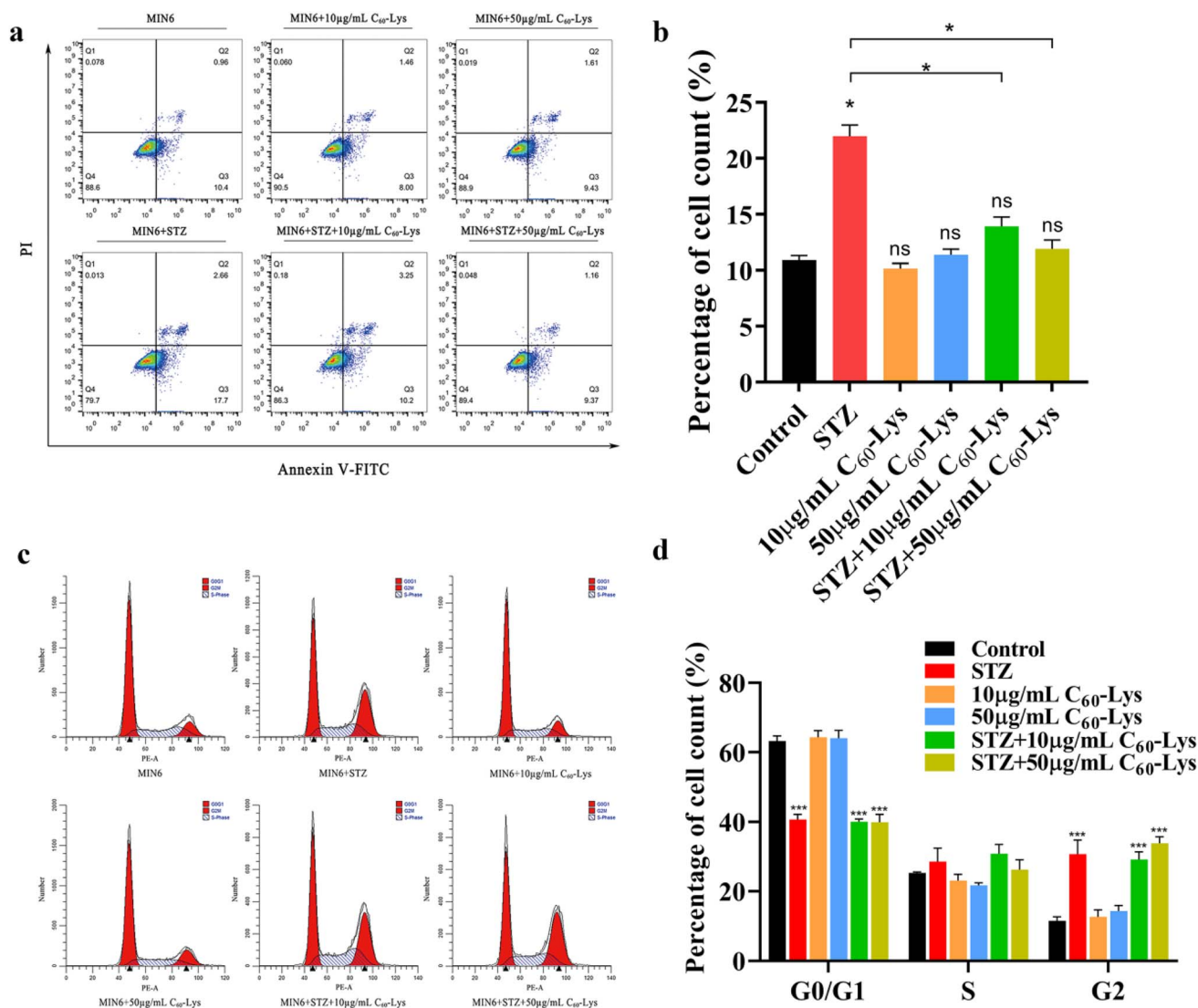
Fig. 3 Cell viability assays *in vitro*. (a) The apoptosis of MIN6 cells, including those treated with C_{60}-Lys. (b) The percentages of apoptotic cells from a. (c) The cell cycle distributions of MIN6 cells, including after C_{60}-Lys treatment. (d) The percentages of cells in each stage from c. ns means $p > 0.05$, * means $p < 0.05$, and *** means $p < 0.001$ compared with the control group. Data were analyzed using t-tests and ANOVA.

It is known that pancreatic β-cells exhibit a reduced antioxidant capacity compared to other metabolic tissue, such as liver and skeletal muscle.[32] Pancreatic β-cells are damaged by the overproduction of ROS. The mitochondrial respiratory chain is the main source of ROS.[33] Mitochondria play a central role in pancreatic β-cell homeostasis and their dysfunction is critical for the development of T2DM.[34] It was determined that the apoptosis of pancreatic β-cells is caused by the overproduction of ROS and oxidative stress.[35] C_{60}-Lys may improve the level of oxidative stress in pancreatic β-cells by stabilizing the mitochondrial membrane potential, thus alleviating pancreatic β-cell apoptosis and maintaining normal cellular physiological function. It could be said that C_{60}-Lys protects pancreatic β-cells by scavenging overproduced ROS. Fullerene derivatives have been extensively studied for direct free radical scavenging applications based on their large numbers of delocalized double π bonds with low-energy unoccupied molecular orbitals

and a large exposed aromatic surface area.[36] They have been called a "sponge for radicals" owing to their effectiveness at scavenging a wide range of ROS, including $O_2^{\cdot-}$, hydroxyl ($^{\cdot}OH$), and lipid radicals.[37]

Excellent anti-T2DM effects in mice

The treatment was conducted for 4 weeks when the mice were 12 weeks old. To assess the therapeutic durability of C_{60}-Lys, the mice were observed for another 3 weeks after stopping drug administration (Fig. 5a). The fasting blood glucose (FBG) levels of the mice were monitored every week during the intraperitoneal injection period (Fig. 5b). The FBG level of T2DM mice was significantly higher than that of the control mice. After the daily administration of C_{60}-Lys for 2 weeks and the observation of C_{60}-Lys treatment in a concentration-dependent manner, the FBG level was reduced in diabetic mice. Interestingly, two and
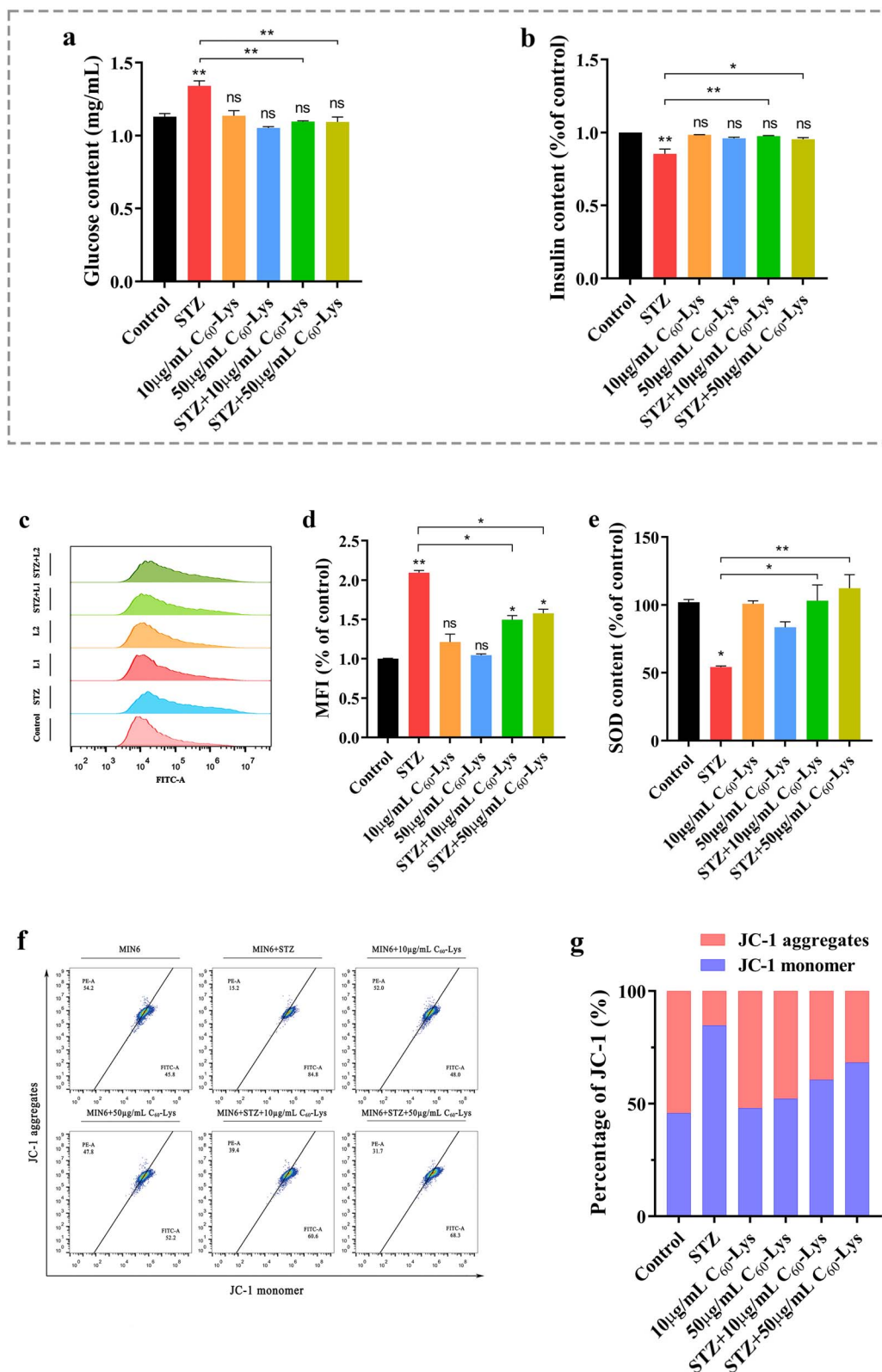
Fig. 4 The effects of C_{60}-Lys on MIN6 cells. (a) The extracellular glucose content of MIN6 cells, including those treated with C_{60}-Lys. (b) The insulin content of MIN6 cells, including those treated with C_{60}-Lys. (c) Intracellular ROS levels in MIN6 cells, including those treated with C_{60}-Lys. (d) The mean fluorescence intensity (MFI) values from (c). (e) The content of SOD in MIN6 cells, including those treated with C_{60}-Lys. (f) Changes in the cellular MMP in MIN6 cells, including those treated with C_{60}-Lys. (g) The percentages of JC-1 monomer and aggregates from f. ns means $p > 0.05$, * means $p < 0.05$, and ** means $p < 0.01$ compared with the control group. Data were analyzed using t-tests and ANOVA.

three weeks after stopping drug treatment, the significantly lower blood glucose level remained for only the high C_{60}-Lys treatment group. It can be inferred that C_{60}-Lys realized a sustainable anti-diabetic effect, and there was no rebound in blood sugar after stopping the administration of C_{60}-Lys. In addition, the body weights of T2DM mice were higher than those of control mice before treatment but C_{60}-Lys could not slow down weight gain in the T2DM mice (Fig. 5c). Meanwhile, the water intake and food intake during the 4 week experiment period were recorded, as shown in Fig. 5d and e. It demonstrated that the diabetic mice treated with C_{60}-Lys took less water. But there was no significant effect on the food intake of the diabetic mice treated with C_{60}-Lys compared with the untreated mice.

From the above results, it is evident that C_{60}-Lys possesses a prolonged pharmacological effect, a distinctive advantage that is currently lacking in other anti-T2DM medications. Furthermore, while metformin may cause lactic acidosis leading to
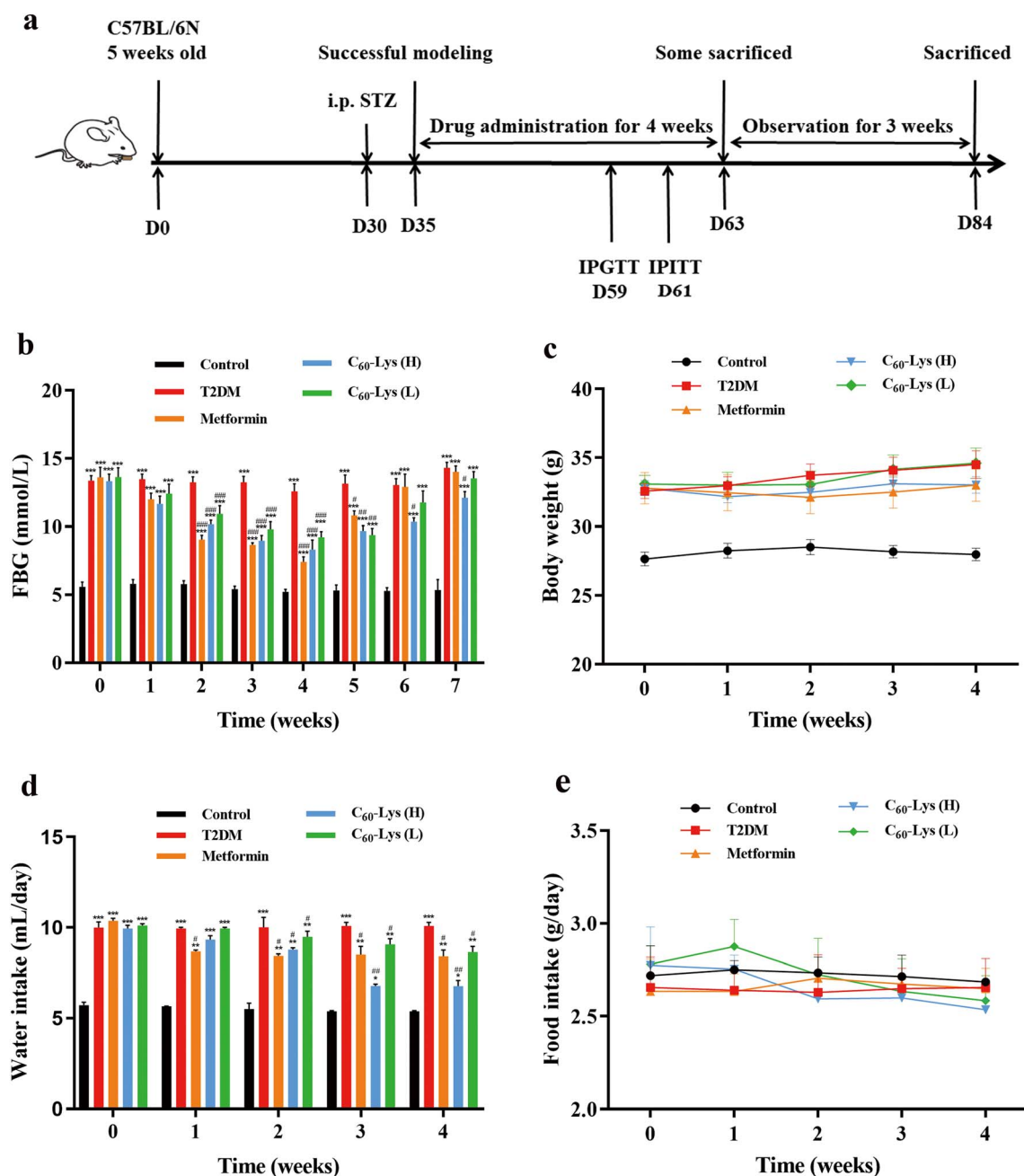

Fig. 5 Anti-diabetic effects of C_{60}-Lys in T2DM mice. (a) The schedule of the animal treatment experimental protocol. (b) The FBG levels of mice during drug treatment for 4 weeks and for 3 weeks after stopping drug administration. (c) The body weights of mice during the treatment. (d) The food intake of mice during the treatment. (e) The water intake of mice during the treatment. * means $p < 0.05$, ** means $p < 0.01$, and *** means $p < 0.001$ compared with the control group. # means $p < 0.05$, ## means $p < 0.01$, and ### means $p < 0.001$ compared with the T2DM group. Data were analyzed using t-tests and ANOVA.

shock[38] and sulfonylureas can result in hypoglycemia,[22] these adverse reactions can be avoided with the use of C_{60}-Lys.

Alleviation of insulin resistance and hyperinsulinemia in T2DM mice

To investigate the effects of C_{60}-Lys on improving insulin resistance, the glucose tolerance after C_{60}-Lys treatment was evaluated by IPGTT on day 59. As shown in Fig. 6a, the fasting blood glucose (FBG) increased rapidly and reached the highest level after about 30 min, and it then gradually decreased with time to stabilize. After 120 min, the FBG of T2DM mice without C_{60}-Lys treatment was significantly higher than that of the control group mice, which indicated that the glucose tolerance of T2DM mice was severely impaired. After C_{60}-Lys treatment, the glucose tolerance of T2DM mice was significantly improved, and C_{60}-Lys was found to improve glucose tolerance in a dose-dependent manner. The area under curve (AUC) values from IPGTT were also quantitatively analyzed, as shown in Fig. 6b. Accordingly, the IPGTT AUC values of C_{60}-Lys treated T2DM mice were significantly reduced compared with the T2DM mice.

To assess the effect of C_{60}-Lys on the improvement of insulin sensitivity in T2DM mice, IPITT was performed in mice after 61 days of drug administration. As shown in Fig. 6c and d, after mice were injected with insulin intraperitoneally, the blood glucose level decreased rapidly and reached the lowest blood glucose within 30–60 min. After 120 min, the fasting blood glucose of mice in the T2DM model group was significantly higher than that in the control group; this indicated that the insulin sensitivity of T2DM mice was severely reduced. The insulin sensitivity of T2DM mice was significantly improved after C_{60}-Lys treatment, and C_{60}-Lys was found to improve insulin sensitivity in a dose-dependent manner. By calculating the AUC values from IPITT, the results showed that C_{60}-Lys could enhance insulin sensitivity in T2DM mice.

The HOMA-IS and HOMA-IR were calculated by measuring the fasting blood glucose level and fasting insulin level in mice. HOMA-IS is an index used to evaluate insulin sensitivity, which increases with an increase in insulin sensitivity. As shown in Fig. 6e, the T2DM mice have a significant decrease in insulin sensitivity. The HOMA-IS in the high-dose C_{60}-Lys treatment group increased 58.18%, while in the low-dose group it increased by 70.69%. It is confirmed that C_{60}-Lys can enhance insulin sensitivity. The level of insulin resistance was evaluated by HOMA-IR. As shown in Fig. 6f, compared with the control mice, the HOMA-IR in the T2DM mice increased significantly. Compared with the T2DM mice, the HOMA-IR in the high-dose C_{60}-Lys treatment group decreased by 58.47%, while in the low-dose C_{60}-Lys treatment group it decreased by 60.40%.

In this work, mice serum was obtained after four weeks of C_{60}-Lys treatment and the insulin level in mouse serum was detected using an enzyme linked immunosorbent assay (ELISA). As shown in Fig. 6g, the serum insulin level in the T2DM mice was significantly increased, and it decreased significantly after C_{60}-Lys treatment. It was clearly seen that C_{60}-Lys could alleviate hyperinsulinemia.

Improving the insulin resistance is the most common method of T2DM treatment.[39] All these results above demonstrated that C_{60}-Lys could improve insulin resistance, resulting in reducing the blood glucose of diabetic mice and effectively improving glucose tolerance. Insulin resistance and hyperinsulinemia are closely associated.[40] It is widely recognized that a dynamic relationship exists between insulin secretion and insulin resistance in which worsening insulin action (*i.e.*, insulin resistance) triggers an increase in insulin secretion, and hyperinsulinemia compensates for the defect in insulin action.[41] Hyperinsulinemia may be initially an adaptation, but it develops as hyperglycemia when the excess demand can no longer be met by overworked β-cells.[38]

## Effects on lipid levels in T2DM mice

T2DM is usually accompanied by hyperlipidemia. The management of diabetic dyslipidemia has been implicated as a key factor in the treatment of T2DM.[42] Therefore the triglyceride (TG) and total cholesterol (TC) levels in mice serum were detected. The results are shown in Fig. 7a and b; the content of TG and TC in the T2DM mice was significantly increased. Compared with the T2DM mice, the TG and TC content after treatment with C_{60}-Lys decreased significantly. It was shown that C_{60}-Lys treatment regulated the lipid metabolism in T2DM mice.

Reversal of pancreatic tissue damage by reducing oxidative stress

In T2DM mice, pancreatic β-cells failed to meet the demands of insulin target organs due to damage from oxidative stress induced by hyperglycemia.[43] Antioxidant enzymes, including SOD and CAT, have always been considered as the first line of defense against free radical damage.[44] As shown in Fig. 7c and d, the SOD and CAT levels in serum were highly decreased in T2DM mice, but significantly increased after treatment with C_{60}-Lys. MDA, an important product of lipid peroxide, was increased in the serum of T2DM mice and it decreased to a non-significant difference after C_{60}-Lys treatment (Fig. 7e); these results indicated that C_{60}-Lys attenuated oxidative stress *via* scavenging ROS and suppressing lipid peroxidation.

The pancreatic index is an objective measure of pancreatic damage and it is used as the simplest indicator to determine the degree of damage and atrophy of pancreatic tissue. The results are shown in Fig. 7f. The pancreatic index of the T2DM mice was significantly lower than that of the control mice; after treatment with C_{60}-Lys, the pancreatic index of mice significantly increased. These results suggest that C_{60}-Lys can improve pancreatic tissue damage in mice.

Given the above evidence, it was hypothesized that C_{60}-Lys treatment could repair the pancreas by improving oxidative stress and decreasing inflammation in T2DM mice. To investigate the restoration of the pancreas by C_{60}-Lys, pathologic analyses were conducted, as shown in Fig. 7g. Obviously, the pancreatic tissue of the T2DM mice was darker in color and smaller in size than that of the control mice, and the cells were irregular, reduced in number and unevenly distributed, accompanied by obvious inflammatory reactions, due to the
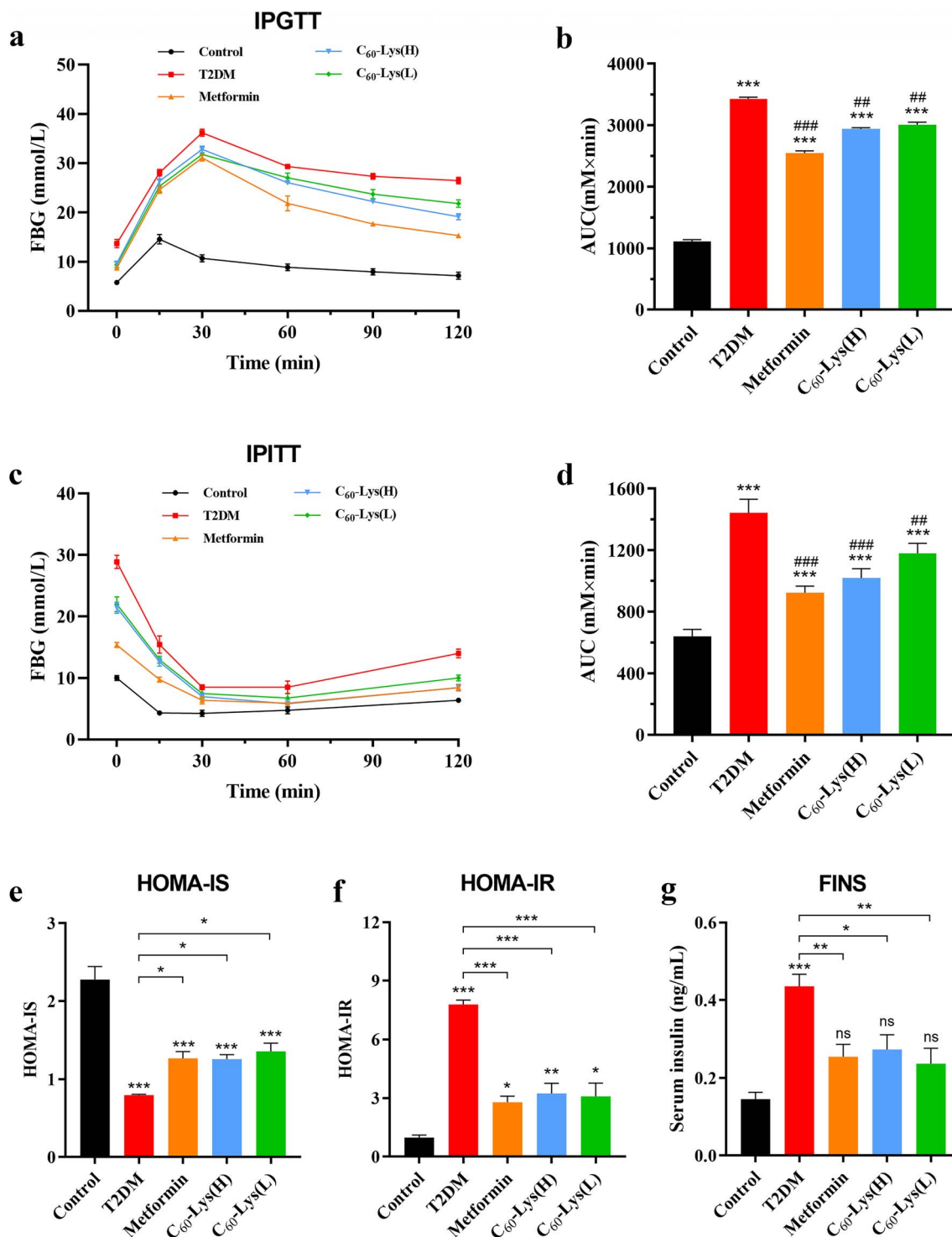
Fig. 6 Anti-diabetic effects of C_{60}-Lys in T2DM mice. (a) IPGTT of mice after 59 days. (b) AUC values from IPGTT after 59 days (c) IPITT of mice after 61 days. (d) AUC values from IPITT after 61 days. (e) The insulin sensitivity index values of mice after treatment. (f) The insulin resistance index values of mice. (g) The mice serum insulin content. ns means $p > 0.05$, * means $p < 0.05$, ** means $p < 0.01$ and *** means $p < 0.001$ compared with the control group. # means $p < 0.05$, ## means $p < 0.01$, and ### means $p < 0.001$ compared with the T2DM group. Data were analyzed using t-tests and ANOVA.

failure of the pancreatic β-cells to compensate for the glucose metabolic load.[45] Most substantially, we found that C_{60}-Lys treatment reversed the abnormal islets of T2DM mice into more regular shapes; the results showed that the islet areas were normalized after C_{60}-Lys treatment. This is also an advantage that distinguishes it from other existing anti-T2DM medications. All the data indicated that C_{60}-Lys could restore the pancreatic damage induced by oxidative stress and maintain
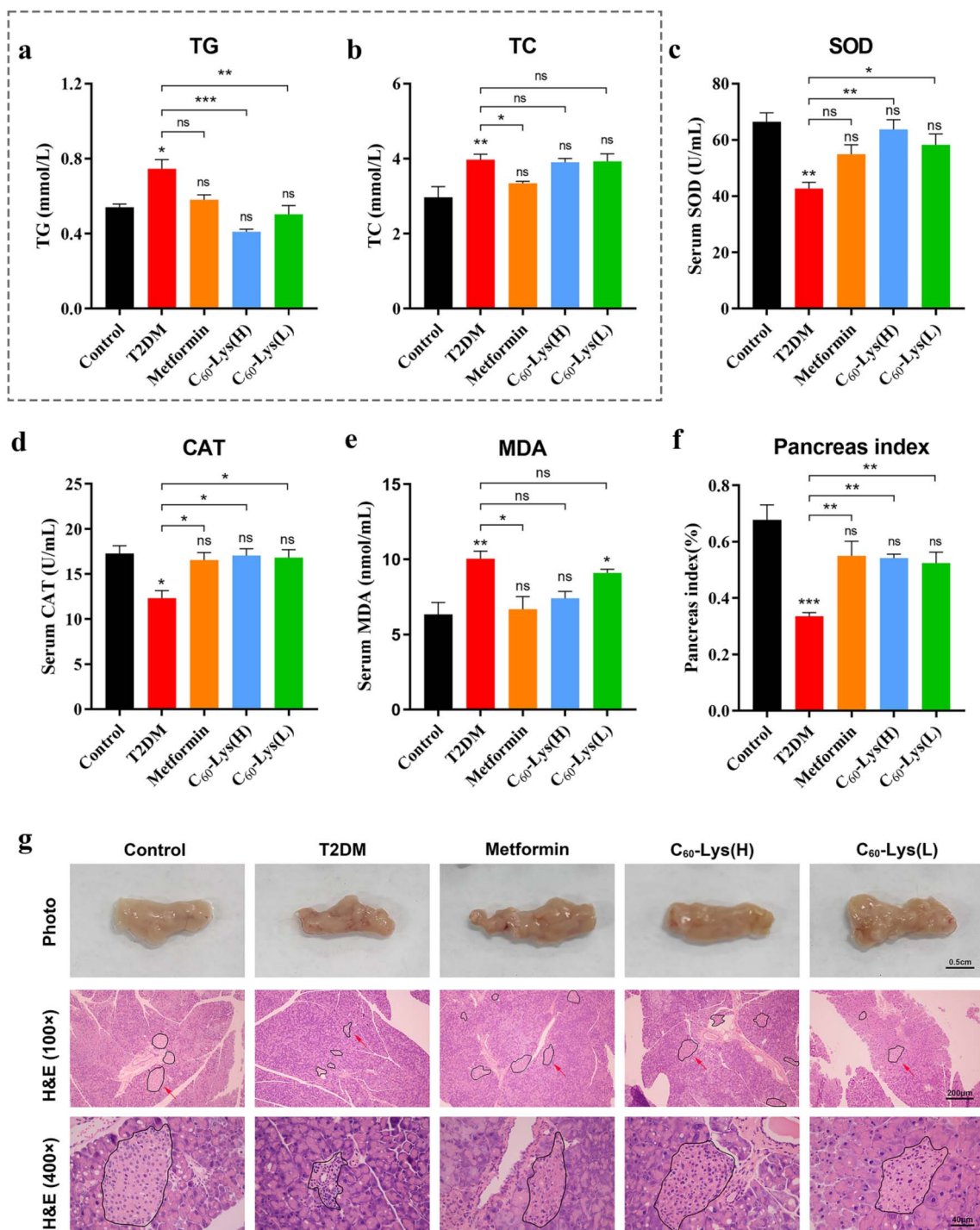
Fig. 7 Reversing pancreatic dysfunction against oxidative stress by 4 weeks of C_{60}-Lys treatment in T2DM mice. (a) The content of mice serum TG. (b) The content of mice serum TC. (c) The content of mice serum SOD. (d) The content of mice serum CAT. (e) The content of mice serum MDA. (f) The pancreatic index values of mice. (g) The pancreatic morphology and H&E staining images. Black circles indicate pancreatic islets. Pictures in the third line are the magnification of the red arrows above. ns means $p > 0.05$, * means $p < 0.05$, ** means $p < 0.01$ and *** means $p < 0.001$ compared with the control group. Data were analyzed by t-test and ANOVA.

pancreatic β-cell functional homeostasis in T2DM mice, eventually normalizing the morphology and secretory function of pancreatic islets. Therefore, the repair of pancreatic islets fundamentally offers the potential to cure T2DM through the use of C_{60}-Lys as an antioxidant agent.

Currently, the majority of commonly used antioxidants possess a limited capacity to scavenge specific types of free radicals.[46] For instance, SOD primarily addresses the removal of superoxide anions ($O_2^{\bullet -}$),[47] while vitamin E is principally involved in the neutralization of lipid peroxyl radicals ($LOO^{\bullet}$).[48]
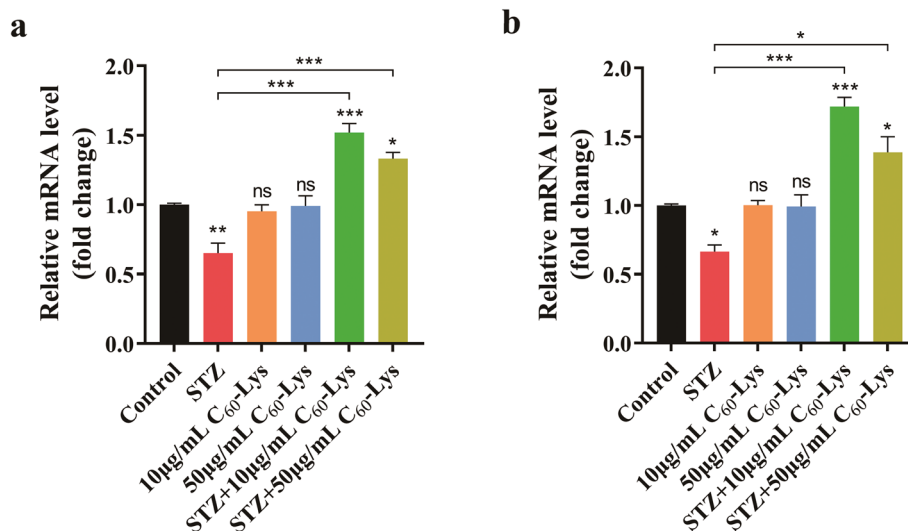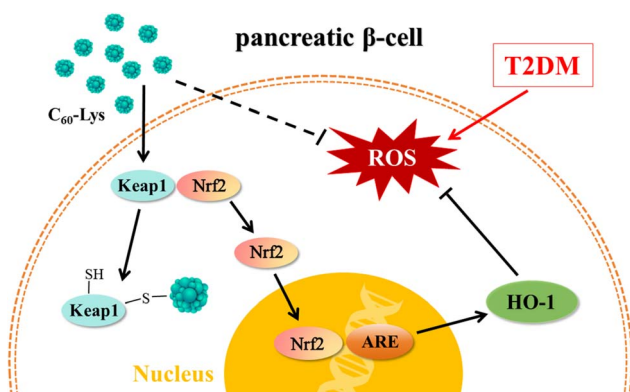
Fig. 8 The expression of oxidative stress-related genes in pancreatic β-cells. (a) HO-1 gene expression, including in C_{60}-Lys-treated pancreatic β-cells. (b) Nrf2 gene expression, including in C_{60}-Lys-treated pancreatic β-cells. ns means $p > 0.05$, * means $p < 0.05$, ** means $p < 0.01$, and *** means $p < 0.001$ compared with the control group. Data were analyzed using t-tests and ANOVA.

Some well-known antioxidants, represented by glutathione (GSH), can prevent damage induced solely by ROS through the inhibition of lipid peroxidation and protein oxidation, but they do not mitigate damage mediated by reactive nitrogen species (RNS).[49] In contrast, fullerene derivatives exhibit a broad spectrum of antioxidant properties; they not only effectively scavenge various types of ROS, including $O_2{}^{\bullet-}$, hydroxyl radicals (${}^{\bullet}OH$) and lipid radicals[50] but they also suppress RNS by directly reacting with nitric oxide.[51] Furthermore, fullerene derivatives demonstrate superior efficacy in free radical scavenging compared to traditional antioxidants.[52]

Upregulation of the expression levels of oxidative stress-related genes in damaged pancreatic β-cells

Increasing evidence has demonstrated that the transcription factor Nrf2 plays a key role in antagonizing oxidative stress.[53] After Nrf2 binds to the antioxidant response element (ARE), it activates the expression of multiple downstream antioxidant genes, such as SOD, CAT and heme oxygenase−1 (HO-1). This

activation helps to improve an organism's oxidative stress status.[54] However, whether the enhancement of the antioxidant enzyme system was a direct response to C_{60}-Lys treatment or a secondary effect from decreasing oxidative stress was still unknown. Therefore, the expression of Nrf2 and HO-1 genes in pancreatic β-cells was measured. As shown in Fig. 8a and b, Nrf2 gene expression and HO-1 gene expression were remarkably reduced in STZ-induced cells but were significantly up-regulated in C_{60}-Lys-treated cells. These results demonstrated that the activation of the Nrf2/ARE/HO-1 pathway is a direct cause of the enhancement of the antioxidant enzyme system upon C_{60}-Lys treatment. According to our hypothesis, C_{60}-Lys may covalently modify the reactive cysteine residues on Keap1, disrupting the nucleophilic interaction between Keap1 and Nrf2.[55] This disruption would lead to the accumulation of Nrf2, allowing it to translocate into the nucleus, where it can bind to ARE and promote the expression of the HO-1 gene. Activating the Nrf2/ARE/HO-1 pathway can reduce ROS (Fig. 9). It was indicated that C_{60}-Lys reduces oxidative stress by increasing the activities of antioxidant enzymes by acting on the Nrf2/ARE/HO-1 signaling pathway.

Conclusions

A kind of novel multifunctional C_{60}-Lys was successfully synthesized, exhibiting excellent hydrophilicity, ROS scavenging capabilities and biocompatibility. After C_{60}-Lys treatment, apoptosis induced by STZ was reduced by 45.84%; SOD enzyme levels were elevated by 107.54%; HOMA-IS was increased by 70.69%; and HOMA-IR was decreased by 60.40% in T2DM mice. C_{60}-Lys was demonstrated to alleviate oxidative stress both *in vitro* and *in vivo*, reversing pancreatic injury and resulting in the restoration of insulin secretion from pancreatic β-cells. This ultimately led to the sustainable reduction of hyperglycemia in T2DM mice. Additionally, C_{60}-Lys also had

Fig. 9 A detailed mechanistic diagram of the C_{60}-Lys activation of the Nrf2/ARE/HO-1 pathway.

a positive effect on lipid peroxidation in T2DM mice, and it can alleviate insulin resistance and hyperinsulinemia. It was strongly suggested that the mechanism of C_{60}-Lys in treating T2DM involves alleviating oxidative stress by acting on the Nrf2/ARE/HO-1 signaling pathway, which increases the activities of SOD and CAT, and stabilizes the MMP of pancreatic β-cells to reduce the overproduction of ROS. All the results indicated that C_{60}-Lys could be a promising avenue for the comprehensive treatment of T2DM and a potential anti-T2DM drug in a clinical setting.

Data availability

Data are available upon request from the authors.

Conflicts of interest

There are no conflicts to declare.

Acknowledgements

References

1 Explore results from the 2019 Global Burden of Disease (GBD) study[EB/OL].

2 E. L. Feldman, B. C. Callaghan, R. Pop-Busui, W. Z. Douglas, E. W. Douglas, L. B. David, B. Vera, W. R. Jamesand and V. Vijay, *Nat. Rev. Dis. Primers*, 2019, **5**, 41.

3 S. K. Gunasekar, L. Xie, A. Kumar, J. Hong, P. R. Chheda, C. Kang, D. M. Kern, C. My-Ta, J. Maurer, J. Heebink, E. E. Gerber and W. J. Grzesik, *Nat. Commun.*, 2022, **13**, 784.

4 M. Wang, Y. Liang, K. Chen, M. Wang, X. Long, H. Liu, Y. Sun and B. He, *Nanoscale*, 2022, **14**, 2119–2135.

5 J. P. Li, Y. Yuan, W. Y. Zhang, Z. Jiang, T. J. Hu, Y. T. Feng and M. X. Liu, *J. Pharm. Pharmacol.*, 2019, **71**, 220–229.

6 J. Chen, Y. Guo, Y. Zheng, Z. Chen, H. Xu, S. Pan, X. Liang, L. Zhai and Y. Q. Guan, *J. Colloid Interface Sci.*, 2025, **684**, 769–782.

7 J. Chiou, C. Zeng, Z. Cheng, J. Y. Han, M. Schlichting, M. Miller, R. Mendez, S. Huang, J. Wang and Y. Sui, *Nat. Genet.*, 2021, **53**, 455–466.

8 H. E. Lebovitz, *Exp. Clin. Endocrinol. Diabetes*, 2001, **109**, S135–S148.

9 G. Dong, S. Adak, G. Spyropoulos, Q. Zhang, C. Feng, L. Yin, S. L. Speck, Z. Shyr, S. Morikawa and R. Kitamura, *Cell Metab.*, 2023, **35**, 332–344.

10 E. Burgos-Morón, Z. Abad-Jiménez, A. M. Marañón, F. Iannantuoni, I. Escribano-López, S. López-Domènech, C. Salom, A. Jover, V. Mora and I. Roldan, *J. Clin. Med.*, 2019, **8**, 1385.

11 N. S. Amirruddin, W. X. Tan, Y. S. Tan, D. S. Gardner, Y. M. Bee, C. S. Verma, S. Hoon, K. O. Lee and A. K. Keong, *Diabetologia*, 2021, **64**, 2534–2549.

12 Q. Huang, Z. Liu, Y. Yang, Y. Yang, T. Huang, Y. Hong, J. Zhang, Q. Chen, T. Zhao and Z. Xiao, *Adv. Sci.*, 2023, **10**, e2300880.

13 Z. Yang, S. Chen, W. Sun, Y. Yang, Y. Xu, Y. Tang, W. Jiang, J. Li and Y. Zhang, *Int. J. Biol. Macromol.*, 2024, **270**, 132249.

14 H. Yaribeygi, T. Sathyapalan, S. L. Atkin and A. Sahebkar, *Oxid. Med. Cell. Longev.*, 2020, 8609213.

15 X. Wang, R. Tian, C. Liang, Y. Jia, L. Zhao, Q. Xie, F. Huang and H. Yuan, *Biomaterials*, 2025, **313**, 122804.

16 T. Tomita, *B. J. Basic. Med.*, 2016, **16**, 162–179.

17 S. Patel, Z. Yan and M. S. Remedi, *Diabetes*, 2022, **71**, 1354.

18 T. Lisa, T. Marco and Z. Yongmin, *Eur. J. Med. Chem.*, 2022, **230**, 114104.

19 H. Ma, J. Zhao, H. Meng, D. Hu, Y. Zhou, X. Zhang, C. Wang, J. Li, J. Yuan and Y. Wei, *ACS Appl. Mater. Interfaces*, 2020, **12**, 16104–16113.

20 S. Lība, Č. Maksims, S. Alīna and M. Modra, *Latvijas*, 2021, **2**, 86–91.

21 H. Zhao, R. Zhang, X. Yan and K. Fan, *J. Mater. Chem. B*, 2021, **9**, 6939–6957.

22 Y. Xie, B. Bowe, A. K. Gibson, J. B. McGill, G. Maddukuri and Z. Al-Aly, *JAMA Intern. Med.*, 2021, **181**, 1043–1053.

23 P. Y. Chu, A. J. Hackstadt, J. Chipman, M. R. Griffin, A. M. Hung, R. A. Greevy, C. G. Grijalva, T. Elasy and C. L. Roumie, *Diabetes Care*, 2020, **43**, 1462–1470.

24 M. Sadeghi, M. Miroliaei and M. Ghanadian, *Int. J. Biol. Macromol.*, 2024, **270**, 132164.

25 A. Muhammad, M. Pietro and A. D. Ralph, *Lancet Diabetes Endocrinol.*, 2024, **12**, 674–680.

26 J. Dowarah and V. P. Singh, *Bioorg. Med. Chem.*, 2020, **28**, 115263.

27 S. Su, M. Zhen, C. Zhou, X. Cao, Z. Sun, Y. Xu, L. Li, W. Jia, Z. Wu and C. Wang, *Adv. Healthc. Mater.*, 2023, **12**, 2202161.

28 H. Wang, L. Li, X. Cao, M. Zhen, C. Wang and C. Bai, *Nano Res.*, 2023, **16**, 12855–12863.

29 F. L. Shen, D. Li, J. H. Guo and J. M. Chen, *Water Res.*, 2022, **223**, 118960.

30 F. Y. Hsieh, A. V. Zhilenkov, I. I. Voronov, E. A. Khakina, D. V. Mischenko, P. A. Troshin and S. H. Hsu, *ACS Appl. Mater. Interfaces*, 2017, **9**, 11482–11492.

31 B. P. Gargari, V. Aghamohammadi and A. Aliasgharzadeh, *Diabetes Res. Clin. Pract.*, 2011, **94**, 33–38.

32 S. Lenzen, J. Drinkgern and M. Tiedge, *FFree Radic. Biol. Med.*, 1996, **20**, 463–466.

33 S. Kasai, S. Shimizu, Y. Tatara, J. Mimura and K. Itoh, *Biomolecules*, 2020, **10**, 320.

34 S. Li and K. Susztak, *Nat. Rev. Neurol.*, 2025, **21**, 77–78.

35 R. K. Al-Ishaq, M. Abotaleb, P. Kubatka, K. Kajo and D. Büsselberg, *Biomolecules*, 2019, **9**, 430.

36 Y. Zhou, J. Li, H. Ma, M. Zhen, J. Guo, L. Wang, L. Jiang, C. Shu and C. Wang, *ACS Appl. Mater. Interfaces*, 2017, **9**, 35539–35547.

37 A. Lichota, I. Piwoński, S. Michlewska and A. Krokosz, *Int. J. Mol. Sci.*, 2020, **21**, 2281.

38 B. Lazarus, A. Wu, J. Shin, Y. Sang, C. Alexander, A. Secora, L. A. Inker, J. Coresh, A. R. Chang and M. E. Grams, *JAMA Intern. Med.*, 2018, **178**, 903–910.

39 Y. Jia, D. Niu, Q. Li, H. Huang, X. Li, K. Li and L. Li, *Nanoscale*, 2019, **11**, 2008–2016.

40 C. A. P. Crofts, C. Zinn, M. Wheldon and G. Schofield, *Diabesity*, 2015, **1**, 34–43.

41 M. Abdul-Ghani and R. A. DeFronzo, *J. Clin. Endocrinol. Metab.*, 2021, **106**, e1897–e1899.

42 J. L. Sánchez-Quesada and A. Pérez, *Endocrinol. Nutr.*, 2013, **60**, 518–528.

43 D. G. Gorasia, N. L. Dudek, P. D. Veith, R. Shankar, H. Safavi-Hemami, N. A. Williamson, E. C. Reynolds, M. J. Hubbard and A. W. Purcell, *J. Proteome Res.*, 2015, **14**, 688–699.

44 S. Esteva, R. Pedret, N. Fort, J. R. Torrella and T. Pages, *Wilderness Environ. Med.*, 2010, **21**, 325–331.

45 C. Rhodes, *Science*, 2005, **307**, 380–384.

46 M. Pellegrini, C. Senni, F. Bernabei, A. F. G. Cicero, A. Vagge, A. Maestri, V. Scorcia and G. Giannaccare, *Nutrients*, 2020, **12**, 952.

47 R. Li, X. Zhou, D. Liu and W. Feng, *Free Radical Biol. Med.*, 2018, **129**, 138–145.

48 L. Li, R. Jin, Y. Li, H. S. Yoon, H. J. Yoon and K. C. Yoon, *Cutan. Ocul. Toxicol.*, 2021, **40**, 350–358.

49 G. Diaz de Barboza, S. Guizzardi, L. Moine and N. Tolosa de Talamoni, *World J. Gastroenterol.*, 2017, **23**, 2841–2853.

50 A. Lichota, I. Piwoński, S. Michlewska and A. Krokosz, *Int. J. Mol. Sci.*, 2020, **21**, 2281.

51 T. Hao, J. Li, F. Yao, D. Dong, Y. Wang, B. Yang and C. Wang, *ACS Nano*, 2017, **11**, 5474–5488.

52 M. Zhao, C. Wang, J. Xie, C. Ji and Z. Gu, *Small*, 2021, **17**, 2102035.

53 I. M. Copple, A. T. Dinkova-Kostova, T. W. Kensler, K. T. Liby and W. C. Wigley, *Oxid. Med. Cell. Longev.*, 2017, 8165458.

54 Z. Wang, S.-O. Ka, Y. Lee, B.-H. Park and E. J. Bae, *Eur. J. Pharmacol.*, 2017, **799**, 201–210.

55 M. J. Bollong, G. Lee, J. S. Coukos, H. Yun, C. Zambaldo, J. W. Chang, E. N. Chin, I. Ahmad, A. K. Chatterjee, L. L. Lairson, P. G. Schultz and R. E. Moellering, *Nature*, 2018, **562**, 600–604.